This full text paper was peer reviewed at the direction of IEEE Communications Society subject matter experts for publication in the WCNC 2009 proceedings.

Analyzing Path Dynamics in Mobile Ad Hoc Networks Using a Smooth Mobility Model

Lifang Guo
School of Telecommunication Engineering
Beijing University of Posts and Telecommunications
Beijing, China

Khaled Harfoush
Department of Computer Science
North Carolina State University
Raleigh, North Carolina

Huimin Xu
School of Telecommunication Engineering
Beijing University of Posts and Telecommunications
Beijing, China

***Abstract*— The characteristics of node-pair paths are a primary consideration in the design of routing protocols in mobile ad-hoc networks (MANETs). Existing research studies on MANET paths focus on their dynamics in the presence of node mobility and ignore the impact of network configuration such as node density and node transmission range. In this paper, we study MANET paths using a smooth mobility model, which complies with the physical law of smooth motion and is sensitive to the change of node velocity over small timescales. Our Study reveals that for paths connecting nodes with slow mobility through a small number of hops, path stability and availability are dominated by network configuration; whereas, for paths connecting nodes with moderate/fast mobility through a large number of hops, they are dominated by node mobility.**

I. Introduction

Node mobility in mobile ad-hoc networks (MANETs) introduce frequent arbitrary variations in the network topology, frequent disconnections/failures of paths between node pairs, and contribute to the complexity in designing reliable routing protocols in MANETs. A study of the dynamic properties of MANET paths is deemed crucial to provide reliable service.

Many research studies have investigated path properties in MANETs [7-11]. Most rely on random mobility models [12], which assume that the speed and the direction of nodes are kept constant within one movement epoch, and that the change in node velocity and direction across consecutive moves are arbitrary. These assumptions are typically unrealistic as they hide the subtle variations in speed and direction of nodes and lead to sudden, sharp changes in speed and direction. Also, as shown in [13], RWP models tend to concentrate nodal presence in the middle of the deployment region due to border effect. This effect tends to increase the density of nodes and increase MANET link lifetime, thus impairing the theoretical and simulation results. Hence, it is desirable to deploy a smooth mobility model, which does not suffer from the above limitations, to analyze MANET path dynamics.

Furthermore, most research studies on path properties in MANETs focus on the impact of node mobility and ignore the influence of the network configuration such as node density and wireless transmission range. These configuration parameters are mostly assigned fixed values in existing studies. However, a change in the value of these parameters leads to a change in path dynamics and a change in the study conclusions. A thorough study of path properties needs to consider the impacts of both node mobility and network parameters.

In this paper, we investigate path properties using (1) a semi-markov smooth (SMS) mobility model which overcomes the aforementioned limitations [2], and (2) we consider the joint effects of node mobility, network configuration, and node-pair distance. We characterize the behavior of a MANET path based on its stability, represented by the expected k-hop path residual lifetime and its availability, represented by the expected k-hop path available time. The knowledge of path stability and availability can serve as the groundwork for understanding MANETs performance under various degrees of system dynamics.

The rest of this paper is organized as follows. In Section II we discuss the critical wireless transmission range for network connectivity. In Section III we introduce the applied SMS mobility model and the node separation distance model as well as analyze the node-pair distance transition rate. In section IV we investigate the path stability and availability properties. We finally conclude in Section V.

II. Critical Transmission Range

The property of "being connected" is one of the essential characteristics of any network, essentially because in a connected network each node can reach any other node whether directly or indirectly through intermediate nodes. As shown in related studies [2, 11], it is desirable to choose network parameters to ensure a connected network most of the study time. In this paper, we study path properties in MANET networks, which are connected with high probability, say $p(con)$=99%. That is as the network is connected during the 99% of the time.

Consider a MANET with n nodes, in which each node has a transmission range R_c , and nodes are uniformly distributed in an area A. The question is: How to ensure that the resulting network topology is connected with a probability $p(con)$ =99%? In other words, what is an appropriate number of nodes n, and an appropriate minimum wireless transmission range per node, which ensure network

978-1-4244-2948-6/09/$25.00 ©2009 IEEE

This full text paper was peer reviewed at the direction of IEEE Communications Society subject matter experts for publication in the WCNC 2009 proceedings.

connectivity with this high probability. Fortunately, the authors in [1] have answered this question using the following equation:

$$R_c(p,n,A) \geq \sqrt{\frac{(\ln n - \ln\ln\frac{1}{p})A}{n\pi}}. \qquad (1)$$

The minimum wireless transmission range per node calculated in above equation is called the ***critical transmission range (CTR)*** denoted by R_c, which represents a lower bound for the radio transmission range that is needed to achieve a connected network with some probability. Clearly, R_c is a function of the three random variables of P, A, and n.

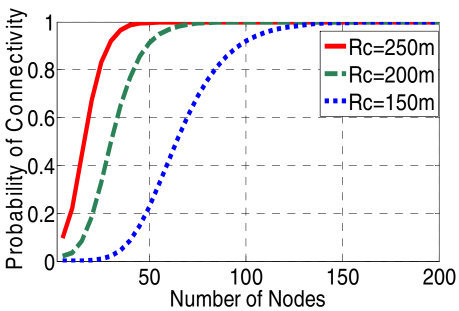

(a) n & $p(con)$

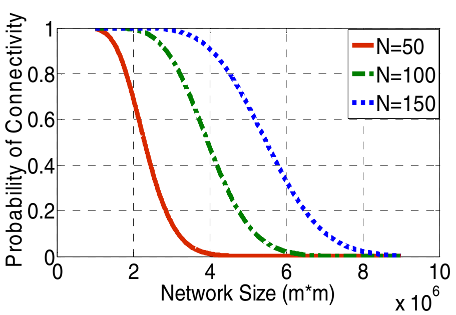

(b) A & $p(con)$

Fig. 1. Network parameters and corresponding $p(con)$

To get a better understanding for this phenomenon, we illustrate it in Figure 1. In Figure 1(a) we use A=1000m*1000m, and plot the connectivity probability as we vary the number of nodes, n, for different values. For example, taking n=50, the connection probability decreases from 1 to 0.91, then dramatically down to 0.23 as the transmission range decreases from 250m to 200m and then to 150m, respectively. In Figure 1(b), using R_c = 350m, when A=2000m*2000m, the MANET network needs at least 100 nodes to ensure $p(con)$=1.

In this paper, we choose n=100, A=1500m*1500m and each node is equipped with an omnidirectional antenna with critical transmission range R_c=257m calculated from equation (1) upon the parameters in order to achieve $p(con)$ =99% which means the entire network being connected during the 99% of entire simulation time.

III. Mobility Characterization in MANETs

This section describes the applied mobility model and node separation distance model used in analyzing the path dynamics. In the end, we discuss the transition rate of node-pair separation distance.

A. *SMS Mobility Model*

A good mobility model should model smooth node movement, capture the tiny variations in node velocity over small time-scales, and should comply with the physical law of smooth motion. In this paper, we use the Semi-Markov Smooth (SMS) mobility model proposed in [2], which satisfies the above mentioned aspects. Specifically, in a mobile scenario, each SMS node movement experiences three consecutive phases: (1) Speed up phase in which a node evenly accelerates its speed from 0m/s to the target speed along a target direction chosen from [0, 2π] ; (2) Middle phase in which a node fluctuates around and in each time step to maintain stable velocity; (3) Slow down phase in which a node evenly decelerates its speed to 0m/s. Then, an SMS movement will be repeated after a random rest time taken from a uniform distribution. Here, Pause time was set to zero, [10, 40] seconds for the moving phase and [4, 8] seconds for acceleration and deceleration phases.

B. *Node Separation Distance Model*

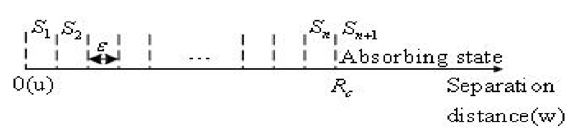

(a). State space with absorbing state

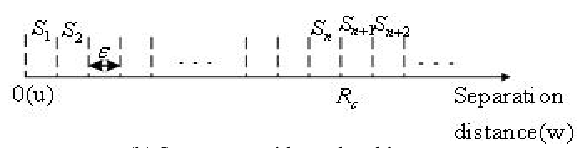

(b) State space without absorbing state

Fig. 2. Node-pair separation distance model.

We use the same node separation distance model as described in [3] to derive the node-pair separation distance transition probability matrix P, which models the node-pair separation distance transition at each time step. In this model, the separation distance between one selected reference node u and the other moving node w that moves into node u's transmission range R_c is divided from 0 to R_c into n bins of width ε , which indicates there are n states denoted by $I = \{S_1, S_2, \cdots, S_i, \cdots S_n\}$ within node u's transmission range, i.e. R_c=n*ε, as illustrated in figure 2. Each element P_{ij} of P represents the transition probability that separation distance is changed from current state S_i to next state S_j after one time step. Here, we assume that the node w enters into the R_c of node u in state i at the first time step and moves out of the R_c of node u first at the m^{th} time step. In figure 2(a) state S_{n+1} is regarded as an absorbing state that represents the u-w separation distance is greater than R_c, used in studying path stability; while in figure 2(b) states $\left\{S_{n+1,} S_{n+2,} \cdots\right\}$ denoting the movement state as u-w separation distance out of the range of R_c are an infinite number of states, used in studying path availability. Therefore, it implies that P is an n+1 by n+1 matrix in the former case and an infinite matrix in the latter case.

The node-pair separation distance transition probability P_{ij} can be derived from [3] as follows:

$$\begin{cases} P_{ij} = \varepsilon \cdot f_{\rho_m|\rho_{m-1}}\left[(j-\frac{1}{2})\cdot\varepsilon \,|\, (i-\frac{1}{2})\cdot\varepsilon \right] \\ f_{\rho_m|\rho_{m-1}} = \int_0^{2(v_\alpha+\delta_v)} \dfrac{\dfrac{\rho_m}{v_\alpha^{\ 2}}\cdot v\cdot e^{\left(\frac{-\pi v^2}{4 v_\alpha^{\ 2}}\right)} dv}{\left[4\rho_{m-1}^{\ 2}\rho_m^{\ 2} - \left[v^2 - \left(\rho_{m-1}^{\ 2}+\rho_m^{\ 2}\right)\right]^2 \right]^{\frac{1}{2}}} \end{cases} ,(2)$$

where ρ_m representing the node-pair distance, v_α denoting the target speed of a node movement and δ_v is the maximum speed variation of v_α in one time step in SMS mobility model [2]. According to [3], taking δ_v =2m/s and ε takes 1m for $v_\alpha \geq 10m/s$; otherwise, $\varepsilon = v_\alpha/10$ m for others v_α.

C. Transition Rate of Node-pair Separation Distance

We next investigate the transition rate of node-pair separation distance to get a deeper understanding of path dynamics for different degrees of node mobility. As shown in Figure 3, the node-pair distance lies in different states as the time t changes.

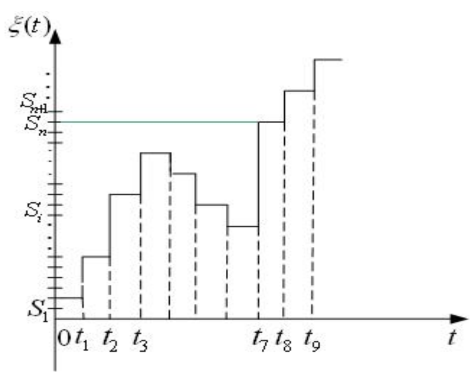

Fig. 3. Node-pair distance transition at different time step.

Recall that P_{ij} $(1 \leq i, j \leq n)$ is the probability of node-pair distance transition from S_i to S_j at a given epoch. Here, we assume that one epoch is one second. $P_{ij}(t) = \left[P^t\right]_{ij}$, which is the transition probability after t epochs between any two states. We explore the transition rate $q(t)$ to learn how fast the transition is, i.e. how frequent the topology changes when we pick different average moving speeds. Hence, the transition rate $q(t)$ of node-pair distance can be expressed as:

$$q(t) = \frac{\text{All the transition probability } \mathrm{P_{ij}(t)}}{\text{All the transition states}}, \quad (3)$$

where $q(t)$ is a function of time t and P is a $n \times n$ matrix. The above equation can be further written as:

$$q(t) = \frac{\sum_{i,j \in I} P_{ij}(t)}{n \times n} = \frac{\sum_{i,j \in I}\left[P^t\right]_{ij}}{n \times n}. \quad (4)$$

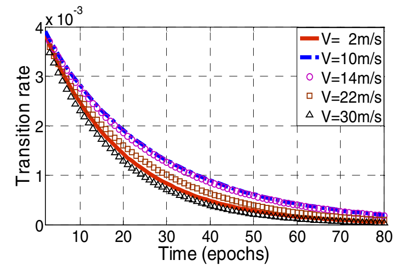

(a) $q(t)$ & time

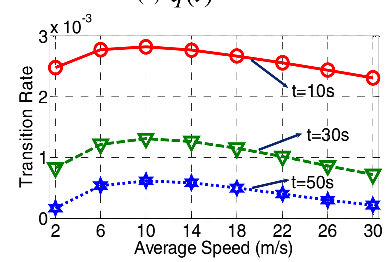

(b) $q(t)$ &V

Fig. 4. The transition rate under the different degree of node mobility.

Figure 4 shows the transition rate under the different degree of node mobility. In figure 4(a), we note that the transition rate exponentially decreases with time regardless of the average moving speeds. For a clearer observation, figure 4(b) plots the transition rate at time 10s, 30s and 50s for the different average moving speed respectively. Interestingly, the figure reveals that the transition rate increases when the average moving speed V is within [2, 10] m/s, while when more than 10m/s, the higher the average moving speed is, the less the transition rate. Thus for low speeds, i.e. below 10m/s, a moving node w spends more time to move out of the transmission range R_c of the selected reference node u; whereas for moderate and high speed, i.e. more than 10m/s, node w spends just a little time to do that. In other words, one moving node w experiences more state transitions to reach out of the transmission range R_c of the selected reference node u for low average moving speed than for moderate and high average moving speed.

IV. Path Properties

In this section, we investigate two important path properties: path stability and path availability due to network configuration, node-pair distance and node mobility. Path stability and availability are important indicators for path selection [4] and for the design of routing algorithms design [5]. Our understanding of path stability and path availability can also serve as the groundwork for understanding MANET performance under various degrees of system dynamics.

In designing path selection algorithm, path residual lifetime (PRL) is taken into account based on the baseline, that is, the selected path has the longest PRL among all the available paths in [4]. Therefore, it implies that the PRL can be used to evaluate how stable the path is. Here, we characterize path stability by the expected k-hop path residual time $\overline{T}_{kPR}$. The k-hop path residual time T_{kPR} is defined as the duration from the time a k-hop path between two nodes is first discovered to the time when one of its constituent links is broken.

To derive the expected k-hop path residual lifetime $\overline{T}_{kPR}$, let us explore the distribution of k-hop path residual lifetime first. Given an active k-hop path between two nodes at time 0, which may also have been active for some time immediately prior to time 0, we assume after m time steps, the node-pair separation distance is in the absorbing state S_{n+1}. Hence, T_{kPR} is a random variable and the CDF of k-hop path residual lifetime is represented by $\Pr\left(T_{kPR} \le m\right)$. For network average mobility metrics, with uniformly distributed nodes, we denote by $P_N^{(0)}$ the probability that at time 0 the initial node-pair distance ρ_0 is in each of states when a new link is formed. The i^{th} element of $P_N^{(0)}$ can be expressed as $P_{Ni}^{(0)} = \Pr(\rho_0 \in S_i, 1 \le i \le n)$; whereas the $(n+1)^{th}$ element is $P_{N(n+1)}^{(0)} = 0\left(i = n+1\right)$, because at time 0 the given link is active, that is, the initial node-pair separation distance must in the state between S_1 and S_n. $P_N^{(0)}$ derived from [7] is a 1 by n+1 row vector whose i^{th} element is

$$P_{Ni}^{(0)} = (2i-1)\frac{\varepsilon^2}{R_c^2}\left(0 \le i \le n\right). \tag{5}$$

Then, we can further derive the CDF of k-hop path residual lifetime denoted by $F_{kPR}(m,k)$ as follows:

$$F_{kPR}(m,k) = \Pr(T_{kPR} \le m) = \left\{\left[P_N^{(0)}P^m\right]_{n+1}\right\}^k, \tag{6}$$

where, P calculated from equation (2) is a n+1 by n+1 matrix. $\left[P_N^{(0)}P^m\right]_{n+1}$ represents the $(n+1)^{th}$ elements of $P_N^{(0)}P^m$, and it means the probability that one communication link of k-hop path breaks, in other words, one node will move out of the transmission range R_c of its reference node in m time steps. From equation (6) the PMF of k-hop path residual lifetime can be written as:

$$\begin{aligned} f_{kPR}(m,k) &= \Pr\left(T_{kPR} = m\right) \\ &= \Pr(T_{kPR} \le m-1) - \Pr(T_{kPR} \le m) \\ &= \left\{\left[P_N^{(0)}P^{m-1}\right]_{n+1}\right\}^k - \left\{\left[P_N^{(0)}P^m\right]_{n+1}\right\}^k. \end{aligned} \tag{7}$$

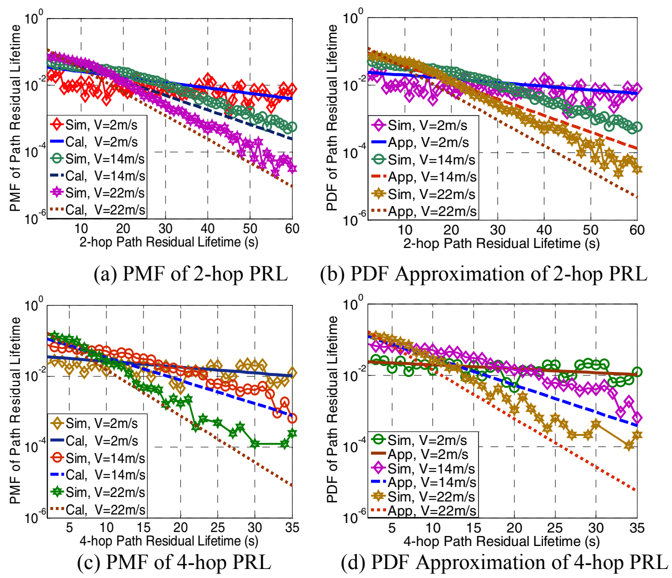

(a) PMF of 2-hop PRL (b) PDF Approximation of 2-hop PRL (c) PMF of 4-hop PRL (d) PDF Approximation of 4-hop PRL

Fig. 5. Distribution of k-hop path residual lifetime.

We observe the calculated and simulation results in figure 5(a) and 5(c), with PMF of the 2-hop path residual lifetime and PMF of the 4-hop path residual lifetime under the different degree of node mobility. In this paper, the average moving speeds V is 2m/s, 14m/s and 22m/s, which represents low speed, moderate speed and high speed respectively. For clear illustration, the figure is plotted in the log-scale on Y-axis. Both calculated and simulation results show that the PMF of k-hop path residual lifetime exponentially decrease with time regardless of the node speed, and the higher average moving speed is, the more quickly it decreases. Meanwhile, by taking a close look, we find that the PMF of k-hop path residual lifetime can be approximated by an exponential distribution function with parameter $\frac{2V \cdot k}{R_c}$ as follows:

$$f_{T_{kPR}}(t) = \frac{2V \cdot k}{R_c} e^{\left(-\frac{2V \cdot k}{R_c}t\right)} = \frac{2V \cdot k}{f(n,A,p)} e^{\left(-\frac{2V \cdot k}{R_c}t\right)}. \tag{8}$$

In order to verify our approximation, the figure 5(b) and 5(d) is again plotted in the log-scale on Y-axis. It is noted that

This full text paper was peer reviewed at the direction of IEEE Communications Society subject matter experts for publication in the WCNC 2009 proceedings.

the PDF approximation fits very well with simulation results especially for nodes with lower average moving speed.

Next, from equation (7) the expected k-hop path residual lifetime $\overline{T}_{kPR}$ is given by:

$$\overline{T}_{kPR} = E(T_{kPR}) = \sum_{m=1}^{\infty} m \times f_{kPR}(m,k)$$
$$= \sum_{m=1}^{\infty} m \left\{ \left\{ \left[P_N^{(0)} P^{m-1} \right]_{n+1} \right\}^k - \left\{ \left[P_N^{(0)} P^{m} \right]_{n+1} \right\}^k \right\}. \quad (9)$$

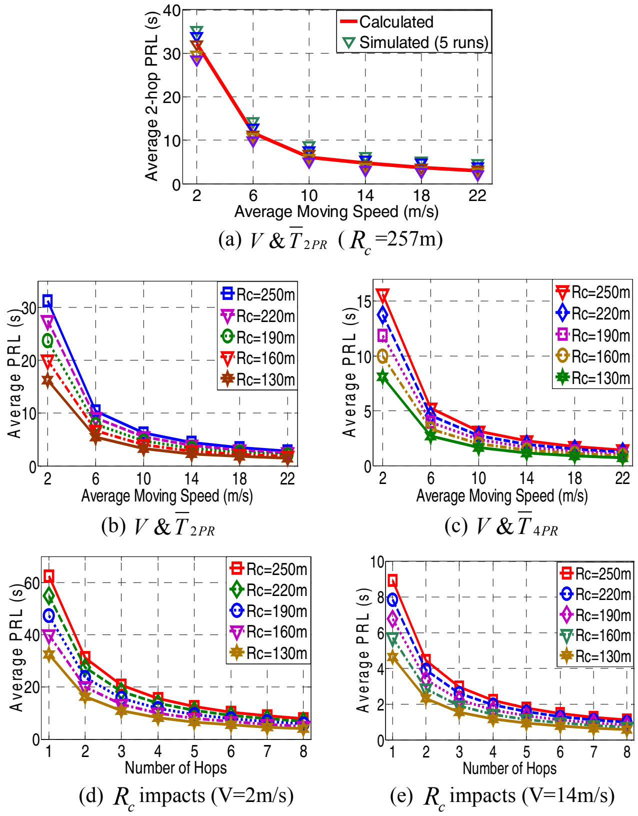

(a) V & $\overline{T}_{2PR}$ (R_c=257m)

(b) V & $\overline{T}_{2PR}$

(c) V & $\overline{T}_{4PR}$

(d) R_c impacts (V=2m/s)

(e) R_c impacts (V=14m/s)

Fig. 6. R_c & V & $\overline{T}_{kPR}$

In figure 6(a), Taking the expected 2-hop PRL $\overline{T}_{2PR}$ as an example, it can be seen that the calculated $\overline{T}_{2PR}$ matches very well with the simulation results. Figure 6(b), 6(c), 6(d) and 6(e) show the impacts of R_c and node mobility on the expected k-hop path residual lifetime $\overline{T}_{kPR}$. In this paper, the value of R_c is selected as 250m, 220m, 190m, 160m and 130m, which corresponds to the network connection probability $P(con)$ being 98%, 88%, 50%, 10% and 0.1% respectively obtained from equation (1). It can be seen that R_c has more significant impacts on shorter hop count and lower average moving speed, and the $\overline{T}_{kPR}$ decreases with R_c, which is consistent with our intuition. It implies that in mobile ad hoc networks, for paths connecting nodes with slow mobility through a small number of hops, the path stability is dominated by the R_c, i. e. network parameters setup; while for paths connecting nodes with moderate/fast mobility through a large number of hops, it is dominated by node mobility.

We also find that $\overline{T}_{kPR}$ can be well approximated by $\widetilde{T}_{kPR} = \dfrac{R_c}{2V \cdot k}$. To justify that, the calculated $\overline{T}_{kPR}$ and the approximated $\widetilde{T}_{kPR}$ are compared in table I with respect to node mobility.

Table I.

THE CALCULATED $\overline{T}_{kPR}$ AND APPROXIMATED $\widetilde{T}_{kPR}$ (R_c =257m)

V (m/s)	2	6	10	14	18	22
$\overline{T}_{2PR}$	32.25	11.65	6.14	4.81	3.74	2.99
$\widetilde{T}_{2PR}$	29.13	9.71	5.83	4.16	3.24	2.65
$\overline{T}_{3PR}$	21.76	7.32	4.10	2.98	2.47	1.98
$\widetilde{T}_{3PR}$	19.42	6.47	3.88	2.77	2.16	1.78

A. *Path Availability*

In this section, we emphasize the analysis of k-hop path availability that is defined as the probability that a k-hop path is available after a certain time. We use the expected k-hop path available time to manifest how available a network topology is. In contrast to previous studies in [8] and [9], we utilize the knowledge of node separation distance related to aforementioned transition probability matrix P in section III to get a more accurate evaluation of path availability.

As mentioned in [7], the path availability is an intermittent mobility metric that means the k-hop path may be broken at time m, but it will be reestablished after this time. Hence, we use the infinite-size transition probability matrix P without absorbing state in section III, in which P_{ij} is the probability of node-pair distance transition from state S_i to state S_j in a given epoch. P satisfies $P_{ij} \geq 0$ and $\sum_j P_{ij} = 1$. Recall equation (5), $P_{Ni}^{(0)} = (2i-1)\dfrac{\varepsilon^2}{R_c^2}(0 \leq i \leq n)$, while $P_{Ni}^{(0)} = 0 (n+1 \leq i < \infty)$.

The probability of one link being in existence after m time steps is the sum of probabilities of all the node-pair separation distance being in one of S_1 to S_n at time step m. Thus, the link availability is the sum of the first n elements of $P_N^{(0)} P^m$ whose the i^{th} element is denoted by $p_{Ai}(m)$. Therefore, the probability A_k that the k-hop path is available at time m is given by:

$$A_k(m,k) = \left[\sum_{i=1}^{n} p_{Ai}(m) \right]^k . \quad (10)$$

Then the expected k-hop path available time $\overline{T}_{kA}$ can be expressed by the following:

This full text paper was peer reviewed at the direction of IEEE Communications Society subject matter experts for publication in the WCNC 2009 proceedings.

$$\overline{T}_{kA}(m,k) = \sum_{m=1}^{\infty} m \times A_k(m,k) . \qquad (11)$$

In figure 7(a) and 7(b), both theoretical and simulated A_k show the higher the node mobility is, the more quickly k-hop path availability decreases. The calculated $\overline{T}_{kA}$ matches very well with simulation results seen from figure 7(c) and 7(d). From figure 7(e), 7(f), 7(g) and 7(h), we find that the k-hop path average available time decreases dramatically when node speed is larger than 10m/s, i.e. moderate or high speed picked. It also indicates that in mobile ad hoc networks, for paths connecting nodes with a slow moving speed through a small number of hops, path availability is dominated by R_c, i.e. network parameters; whereas for path connecting nodes with a moderate or fast mobile speed through a large number of hops, path availability is dominated by node mobility.

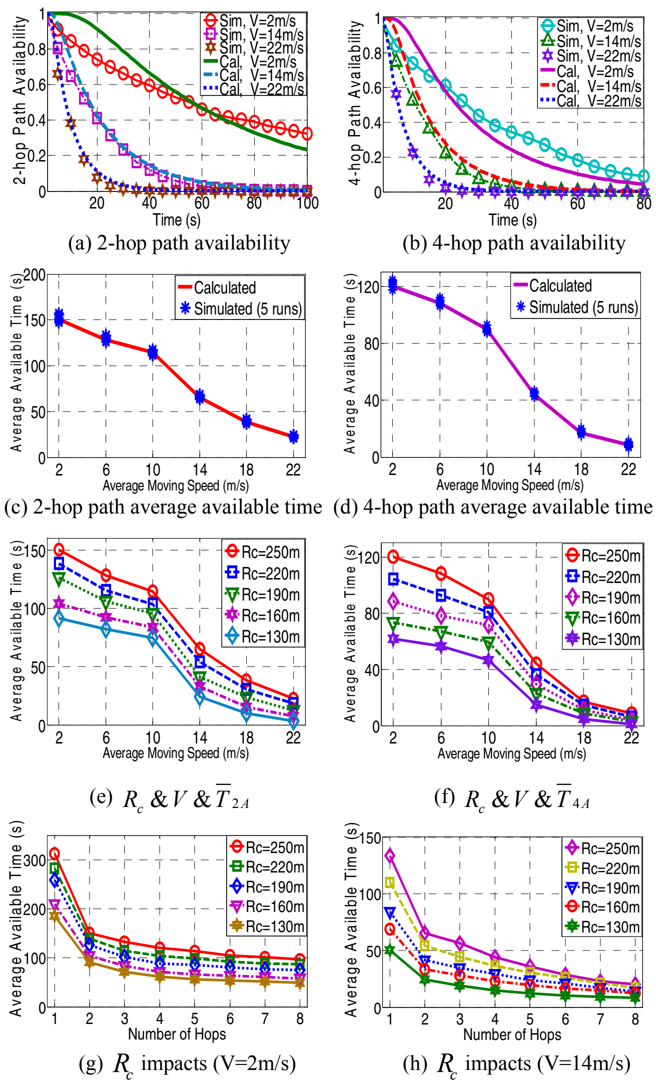

(a) 2-hop path availability (b) 4-hop path availability

(c) 2-hop path average available time (d) 4-hop path average available time

(e) R_c & V & $\overline{T}_{2A}$ (f) R_c & V & $\overline{T}_{4A}$

(g) R_c impacts (V=2m/s) (h) R_c impacts (V=14m/s)

Fig7. The impacts of R_c and node mobility V on k-hop Path availability and the expected k-hop path available time

V. CONCLUSIONS

In this paper, we have laid the ground for understanding path dynamics in MANETs through closed-form analysis. As opposed to earlier studies, our analysis relies on a smooth mobility model and takes into consideration the joint impacts of node mobility, node density, wireless transmission range, and node-pair distance. We reveal that in MANETs, for paths connecting nodes with a slow moving speed through a small number of hops, path stability and availability are dominated by network configuration; whereas for path connecting nodes with a moderate/fast mobile speed through a large number of hops, they are dominated by node mobility. Our study can be used to evaluate MANET routing protocols, to measure MANET performance, and to enhance our understanding of ad-hoc topology dynamics.

REFERENCES

[1] C. Bettstetter, "On the Connectivity of Ad Hoc Networks," *The Computer Journal*, Vol. 47 No. 4, 2004, pp. 432-447.

[2] M. Zhao and W. Wang, "A novel semi-markov smooth mobility model for mobile ad hoc networks," in *Proc. of IEEE GLOBECOM*, Nov. 2006, pp. 1-5.

[3] M. Zhao and W. Wang, "Analyzing topology dynamics in ad hoc networks using a smooth mobility model," in *Proc. of IEEE WCNC*, 2007.

[4] E. Y. Hua and Z. J. Haas, "Path selection algorithms in homogeneous mobile ad hoc networks," in *Proc. ACM IWCMC*, 2006, pp. 275-280.

[5] M. Yu, A. Malvankar and S. Y. Foo, "An energy-efficient path availability routing algorithm for mobile ad hoc sensor networks," in *Proc. of IEEE ICC*, June 2006, pp. 1885-1890.

[6] http://www.ietf.org/rfc/rfc2501.txt

[7] S. Xu, K. L. Blackmore and H. M. Jones, "An analysis framework for mobility metrics in mobile ad hoc networks," in *EURASIP Journal on Wireless Communications and Networking*, 2007.

[8] D. Yu, H. Li and I. Gruber, "Path availability in ad hoc networks," in *Proc. of IEEE ICT*, 2003, pp. 383-387.

[9] B. McDonald and T. Znati, "A path availability model for wireless ad hoc networks," in *Proc. of IEEE WCNC*, 1999, pp.35-40.

[10] F. Bai, N. Sadagopan, B. Krishnamachari and A. Helmy, "Modeling path duration distributions in MANETs and their impact on reactive routing protocols," *IEEE Journal on Selected Areas in Communications*, September 2004, pp. 1357-1373.

[11] R. J. La and Y. Han, "Distribution of path durations in mobile ad hoc networks and path selection," *IEEE Transactions on Networking*, 2007, pp. 993-1006.

[12] T. Camp, J. Boleng, and V. Davies, "A survey of mobility models for ad hoc networks research," *Wireless Communication and Mobile Computing (WCMC): Special issue on Mobile Ad Hoc Networking: Research, Trends and applications*, 2002, pp. 483-502.

[13] C. Better, G. Resta and P. Santi, "The node distribution of the random waypoint mobility model for wireless ad hoc networks," *IEEE Transactions on Mobile Computing*, 2003, pp. 257-269.

[14] M. K. Marina and S. R. Das, "On-demand multipath distance vector routing in ad hoc networks," in *Proc. of Intern. Conf. for Network Protocols (ICNP)*, (Riverside, CA), November 2001.

[15] Jain, R., Puri, A. and Sengupta, "Geographical routing using partial information for wireless ad hoc networks," in *Proc. of IEEE Pers. Commun. Mag.*, pp. 48-57, August 2001.